ELSEVIER

International Journal of Mass Spectrometry 215 (2002) 89–100

International Journal of Mass Spectrometry

www.elsevier.com/locate/ijms

High resolution focal plane detector for a space-borne magnetic mass spectrometer

Jean-Jacques Berthelier[a,*], Jean-Marie Illiano[a], Dennis Nevejans[b], Eddy Neefs[b], Etienne Arijs[b], Niels Schoon[b]

[a] *CETP/IPSL, 4 Avenue de Neptune, 94100 Saint-Maur, France*
[b] *BIRA-IASB, Ringlaan 3, B-1180 Brussels, Belgium*

Received 25 September 2001; accepted 4 December 2001

Abstract

A detector system has been designed to meet the specifications of the focal plane detector for the double focusing mass spectrometer (DFMS) which is part of the ROSINA experiment to be flown on board the ESA Rosetta orbiter. This spacecraft will be launched in January 2003 and aims at a rendezvous with comet Wirtanen in 2011. In the first section, the specifications of the detector system are defined as a function of the desired measurements and instrument characteristics. The main component is an imaging detector, the design and rationale of which are described in the second section. The main characteristics are a very high resolution of 25 μm per pixel and a large dynamical range of about 11 decades. In the last section, initial results from laboratory tests of a prototype are provided together with an overview of the actual performances. In conclusion, work anticipated in the future and possible improvements are summarized. (Int J Mass Spectrom 215 (2002) 89–100) © 2002 Elsevier Science B.V. All rights reserved.

Keywords: Focal plane detector; Mass spectrometer; MCP; Imaging techniques; Planetary instrumentation

1. Introduction

The detector system described in this paper has been designed to meet the specifications of the double focusing mass spectrometer (DFMS) which is part of the ROSINA experiment to be flown on board the ROSETTA orbiter. ROSETTA, the third cornerstone mission of the ESA scientific program, will be launched in January 2003 and aims at a rendezvous with comet Wirtanen in 2011 [1]. The orbiter will accompany the nucleus along its orbit from about 3.5 AU (astronomical units) from the sun at the time of the rendezvous to a heliocentric distance of 1 AU at perihelion. The main goals of this ambitious mission are to study the structure and properties of the nucleus and its outgassing, as well as the formation and evolution of the cometary atmosphere as it evolves from a very tenuous gaseous envelope far from the sun to a fully developed coma at perihelion. Among the various instruments carried by the scientific payload, the ROSINA experiment aims at studying the cometary atmosphere. Its objectives are to determine the elemental, chemical and isotopic composition of the neutral and ionized gas and to study its temporal evolution and dynamics. This new set of observations

* Corresponding author.
E-mail: jean-jacques.berthelier@cetp.ipsl.fr

1387-3806/02/$20.00
PII S1387-3806(02)00527-4

will, in particular, allow a new insight into the nature and formation of comets. Such objects are considered as the most pristine objects in the solar system and are assumed to have kept a record of the physical and chemical conditions that prevailed at the early stage of condensation of the solar nebula. Composition measurements will also provide information of their relation with interstellar matter, while temporal evolution of the neutral and ionized gas species will allow the study of processes which govern the outgassing of the nucleus and the interaction of the cometary atmosphere with the solar wind.

The ROSINA experiment [2] combines two complementary mass spectrometers to analyze the composition of the cometary neutral and ionized gas and two density gauges to measure its local pressure and radial flow velocity. One mass spectrometer (RTOF) is a time-of-flight instrument with a mass range of 1–300 amu, and a mass resolution $m/\Delta m > 500$ at 1%, the other one, DFMS, is a double focusing magnetic mass spectrometer with a reduced mass range from 12 to 100 amu, but specifically designed to provide a high sensitivity and a mass resolution $m/\Delta m > 3000$ at 1%. Ion sources of both instrument have a sensitivity of 10^{-7} A/Pa.

In this paper we describe the detector system which has been developed to equip the focal plane of DFMS. In Section 2, a brief description of the desired measurements together with the main characteristics of the instrument allows the specifications of the detector to be defined. Section 3 presents the detector concept, its rationale and a description of the prototype unit. In Section 4, initial results from laboratory tests and an overview of the performances are given. We shall summarize in conclusion the tests that are in progress and in Section 6 the work which is anticipated in the future to accompany the development of the detector and its possible improvements.

2. The DFMS objectives and requirements

The DFMS is an optimized Mattauch–Herzog double focusing magnetic mass spectrometer which has been developed at the Physikalisches Institut of the University of Bern in Switzerland. There are two modes of operation, respectively, the neutral mode and the ion mode. In the neutral mode particles are first ionized in the ion source. Then, they pass through an object slit before being accelerated by the DFMS mass-dependent accelerating potential to the entrance of a toroïdal electrostatic analyzer followed by a magnetic sector. The geometry of these two analyzers has been optimized in order to provide second-order focusing of ion trajectories in a focal plane at the exit of the instrument. A multipolar lens system located between the exit face of the magnet and the focal plane provides a zooming capability, allowing control of the separation of adjacent mass peaks in the focal plane. This feature allows variation of the instantaneous mass range being analyzed by the spectrometer and, consequently, its effective mass resolution. Ionization is done via an electron bombardment source, that uses a heated tungsten filament as electron emitter, having an efficiency equal to 10^{-7} A/Pa. In the ion mode, the ionization source is powered off. A detailed description of the DFMS instrument can be found elsewhere [2].

The main requirements for the detector of the DFMS come from the set of conditions which will be encountered in the environment of comet Wirtanen during the operational phase of the mission [1] and from the characteristics of the mass spectrometer itself. While the distance to the sun decreases from $\sim$3.5 to $\sim$1 AU, the outgassing rate of the comet nucleus is expected to increase by about five orders of magnitude, from $\sim 10^{24}$ to $\sim 10^{29}$ molecules per second. The gas density at a fixed distance from the nucleus will change accordingly, but one has also to take into account about two orders of magnitude of change in the local gas density due to the planned variations of the distance between the nucleus and the orbiter. Finally, the instrument must also be able to detect minor species with a mixing ratio of $\sim 10^{-3}$. Hence, the total dynamical range for neutral measurements is about 10 orders of magnitude and the desired sensitivity threshold in the neutral mode corresponds to a pressure of 10^{-15} Pa. From various models for

the ion production, chemistry and dynamics in the inner coma, ion densities from 10^1 to 10^5 ions/cm^3 have been estimated in [3]. Again the mixing ratio of minor species has to be taken into account, in particular in the case of rare isotopes like ^{13}C, ^{17}O, ^{18}O the measurement of which will be mostly performed in the ion modes which provides a much higher sensitivity and thus allow for measurement times of the order of minutes. This gives a desired dynamical range of approximately nine orders of magnitude in the ion modes. Considering the various modes of operation, the varying conditions in the coma and the desired sensitivity of the instrument, the detector must allow measurement of ion fluxes from 10^{-1} to 10^{10} ions/s per mass peak. As far as the instantaneous dynamical range is concerned, already mentioned values of the relative density of minor constituents or of rare isotopes which are detected simultaneously have been taken as a guideline, calling for a value of better than 10^3.

Another major requirement comes from the mass resolution and the optical properties of the spectrometer. Among the scientific objectives associated with gas composition measurements in a cometary atmosphere, at least two call for a very high mass resolution. The first one is the need to separate $^{12}C^{16}O$ and $^{14}N_2$, with respective masses of 27.994 and 28.005 amu, which are records of the origin and processes of formation of the nucleus. The second one is the precise determination of the isotopic ratio of carbon, which calls for separation of ^{13}C from ^{12}CH with respective masses of 13.003 and 13.008. Density ratios between N_2 and CO or ^{13}C and ^{12}CH may be variable but expected values require that the instrument provides a mass resolution $m/\Delta m$ of $\sim$2500 down to a few percent of the most abundant mass peak.

Finally two other requirements must also be taken into account. First, for a mission with a 10-year duration like ROSETTA, the guaranteeing of absolute calibration of the measurements asks for an in-flight calibration of the gain of particle detectors such as channeltron electron multipliers (CEM) or micro-channel plates (MCP), which are known to vary as a function of aging and integrated count rate. The second stems from reliability considerations, of paramount importance for this long duration space mission, especially in the potentially detrimental dusty environment of the comet nucleus. Together with the usually imposed constraints on materials and allowed component voltages, the requirement for the detector system was thus to provide as much as possible redundant measurements of similar quality.

3. Detector concept and description

The neutral and ionized gas density and composition in the coma region of the comet may undergo significant time variations: for the neutral gas these are due to outgassing bursts and, for the cometary ions, to changes of the extension and position of distinct coma regions, the boundaries of which may sweep rapidly through the position of the spacecraft in response to solar wind variations [4]. In the absence of previous measurements, the characteristic times of these variations are practically unknown. Outgassing bursts could occur over tens of seconds, while temporal changes of boundaries in the ionized coma may results in faster, $\sim$1 s, local perturbations. For this reason it was decided to build a detector with an imaging capability to measure simultaneously a large enough range of masses and reduce accordingly the duration of measurements. Evidently, this is also extremely important for measurements of adjacent isotopes with very large differences in density: when they are measured in a single sequence, their measured ratio is unaffected by variations of the cometary atmosphere.

The central part of the detector system is thus an imaging detector using a MCP followed by a specially designed collector, the LEDA 512, which provides the required image resolution. To answer the two last requirements of absolute calibration and redundancy two other detectors where added: a Faraday cup measuring the total current of the most abundant water peaks (H_2O in the neutral mode and H_3O^+ in the ion mode), and a CEM preceded by a narrow slit to perform measurements with a similar mass resolution as that of the MCP, by using a sequential scan over the various mass peaks to provide the mass spectrum.

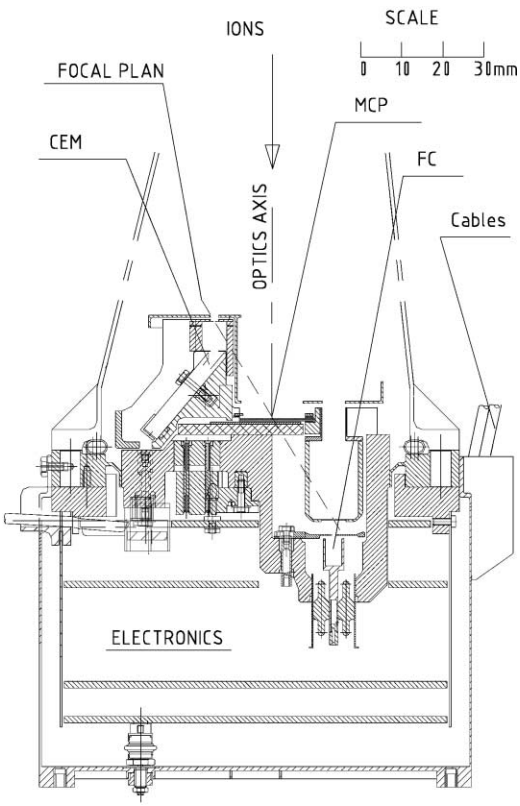

Fig. 1. Schematic view of the DFMS detector system. The position of the CEM, imaging detector and Faraday cup are readily seen on this cut of the detector flange through its plane of symmetry (see the text for more details).

The complete detector system is shown in Fig. 1. The broken line indicates the location of the theoretical focal plane of the spectrometer; it is inclined at 31° with respect to the central axis of the ion beam exiting from the magnet. The MCP is perpendicular to the central axis of the ion beam, thus at an angle of 59° with respect to the focal plane. This orientation, which is not optimal, results in a slight deterioration of the sharpness of the mass peaks. This effect remains insignificant in practice because ions that focus on the focal plane have trajectories that make very shallow angles with the central axis of the beam. Such an orientation of the MCP was necessary because ions exiting from the source are accelerated at the entrance of the ion optics to a potential that varies as the reciprocal of their mass. When the spectrometer is set to detect high mass ions (e.g., $m/z = 100$), their energy at the exit of the magnet is only ∼600 V, a level which corresponds to a very low efficiency of detection by the MCP. The ions need thus to be accelerated to a higher energy before impinging on the MCP and this is obtained by polarizing the front face of the MCP at −3 kV with respect to the DFMS potential. To minimize the disturbances of the ion trajectories, the accelerating electric field must be aligned with these trajectories, hence the need to have the MCP perpendicular to the central ray of the ion beam.

The CEM is located 15 mm off-axis in the focal plane, on the left of the MCP as shown in Fig. 1; its entrance slit is at the DFMS accelerating potential. At this location, the focal properties of the DFMS ion optics are only slightly degraded compared to near the central axis and the mass resolution is still compatible with the specifications. The CEM can operate in two modes of operation, pulse counting and direct current measurement, to allow for a dynamical range similar to the MCP. On the right side of the MCP and below it, at a similar off-axis distance as the CEM, is positioned the entrance slit of the Faraday cup (FC). Before entering the Faraday cup, ions travel through a box that is electrically connected to the local floating detector potential. It has a 5.5 mm wide entrance, large enough not to intercept any ion trajectory that focuses on the entrance slit of the cup. This grounded box provides an electrostatic shield against high voltages applied to the near-by MCP, which would otherwise disturb the ion trajectories that are focused on the Faraday cup entrance. Measured currents span from 10^{-15} to 10^{-8} A in three sensitivity ranges with some partial overlapping between them; the settling time of the FC electrometer is about 1 s to 0.01% of full-scale.

The three detectors, MCP and its associated LEDA 512, CEM and FC, are mounted on a ceramic plate with vacuum proofed electrical connections to the other face of the plate. The very complex shape and high accuracy of the ceramic plate together with its high mechanical, thermal and electrical performances required a significant effort during the design and fabrication. The plate itself is brazed on a titanium

flange and the latter is bolted onto a mating flange that is part of the DFMS structure. Between both flanges, a metallic joint ensures the airtightness so that the detector side of the ceramic plate, as well as the entire ion optics and the ion source, can be maintained under a very good vacuum when the instrument is sealed before launch. The detector electronics, which are a significant source of outgassing, are therefore mounted on the other side of the ceramic plate at ambient pressure thus protecting the internal part of the instrument (ion optics and ion source) against contamination. This approach is also necessary when the internal part of the instrument is baked out under vacuum at a high temperature of ∼120 °C.

4. The imaging detector

Since the advent of MCPs, a very large number of techniques have been developed to build one- or two-dimensional imaging detectors [5–11]. A large number of them use MCPs in a pulse mode and rely on resistive or split collectors with two to four outputs. An electronic analysis of the pulses coming out of these outputs allows the determination of the location of the particle impact. Other detectors use a multianode or pixelized collector to measure the spatial distribution of the charges exiting the MCP and thus, determine the one- or two-dimensional distribution of the particle influx on the MCP which can be operated in an analog or in a pulse mode. Recent papers have dealt with the performances of such systems, in particular for spectra measurements [12–14]. In some cases [15], one-dimension detectors use a combination of pulse operation for low counting rates and analog measurement for higher fluxes.

In the case of low counting rates, not in excess of the safe operation limit of about 10^6 counts/(cm^2 s) for MCPs in a pulse mode, the digital technique appears to be the simplest and most accurate solution with a spatial accuracy of about 0.2 mm. However, in the case of the DFMS detector, the need for a dynamical range of more than 11 decades, in combination with measurement times of less than 1 s, preclude the use of a digital technique which would be limited to about seven decades due to the limit on the counting rate and the noise level of 0.1 counts/(cm^2 s).

For this reason we decided to use an analog technique with a multianode collector similar to the detector that the first two authors have built for the neutral mass spectrometer experiment on board the ESA Giotto probe [16]. In this earlier experiment we used a collector in the form of an application-specific integrated circuit (ASIC) consisting of 64 anodes, each having a width of 375 μm, a height of 5 mm and a pitch of 400 μm, and including the charge reading electronics (EG&G RETICON, CA, USA). The major difference with the present detector comes from (i) the required spatial resolution of the detector of 25 μm to cope with the focal plane separation of 350 μm for two adjacent mass peaks such as CO and N_2 at the maximum resolution of DFMS; (ii) the requirement to maintain this mass resolution at 1% of the maximum peak height which poses a very tight constraint on the sharpness of the detection of the electron packet exiting from the MCP. In designing the detector and defining the specifications of the ASIC circuit used as a collector we made use of the extension of more than 16 mm of the focal lines in the focal plane of the DFMS in a direction perpendicular to the plane of symmetry of Fig. 1. We therefore decided to build an ASIC circuit incorporating two identical and totally independent circuits each with 512 anodes, 22 μm wide and 8 mm high, separated from each other by a gap of 3 μm. This ASIC collector covers thus an active area of 12.5 mm × 16 mm and the two independent collectors each with their own reading electronics provide a very satisfactory answer to the reliability requirement. The ASIC collector was designed and fabricated by IMEC (Leuven, Belgium) under the name of the LEDA 512, standing for linear electron detector array with 512 pixels; it is described in detail in this special issue [17].

The MCP is composed of two identical 0.33 mm thick plates with straight channels having a diameter of 6 μm and an inclination of 13°; they are mounted in the chevron configuration with the plane of the

channels perpendicular to the length of the focal plane. These plates are manufactured by Photonics (Brive, France), for night vision instruments. A typical gain vs. voltage curve for the MCP is given in Fig. 2. A maximum gain of $\sim 2 \times 10^6$ is obtained for voltages across the MCP above $\sim$1800 V and the gain varies exponentially with voltage from 5×10^{-2} at 800 V to 6×10^3 at 1300 V. Electrons exiting from the MCP are collected on the LEDA anodes and the accumulated charges are read sequentially and transformed to proportional voltage pulses by the LEDA internal electronics. They are then digitized by a 12 bit ADC that provides the adequate instantaneous dynamical range of better than 10^3 according to the LEDA noise measurements [17]. The gain curve of the MCP shows that a range of eight decades can be easily obtained, taking into consideration that the MCP can operate reliably at a gain less than 0.1 for high ion fluxes. With the 10^3 instantaneous dynamical range provided by the LEDA and ADC, the overall dynamics of the imaging detector amounts to $\sim$11 decades as required by the specifications.

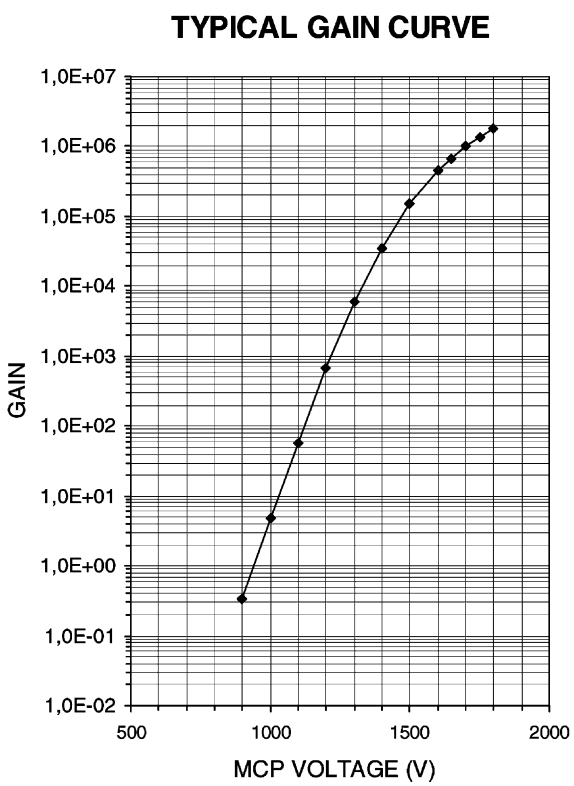

Fig. 2. Gain vs. voltage characteristics of the assembly of 6 μm pore size MCP used in the imaging detector.

The elementary reading time of the LEDA 512 is 6.55 ms. This defines the maximum temporal resolution of the detector, again more than adequate for the instrument. The reading sequence of the charges accumulated on the 512 pixels can be controlled in two ways. First the integration time, which is defined as the time between two LEDA readouts, can be varied from 6.55 ms to $4095 \times 6.55\,\text{ms} = 26.84\,\text{s}$. If one takes into account the leakage current of the LEDA anodes, the practical limit at room temperature is in the order of $\sim 256 \times 6.55\,\text{ms} = 1.6\,\text{s}$. Anyway, leakage current of either sign, which results in charging or discharging of the anodes, can be measured with a great accuracy. This provides a way to correct the measurements and extend the integration time beyond the already mentioned limit. A second possibility, called accumulation or coherent integration, is offered by the field programmable gate array (FPGA) which acquires the digitized data sent by the ADC. A number from 1 to 4095 readings can thus be coherently summed. This allows reduction of the incoherent statistical noise of the LEDA and enhances the effective sensitivity and dynamical range of the detector.

Electron packets exiting from individual channels on the back face of the MCP diverge because they are emitted from various locations on the channel wall near the exit of the channel and also due to the diverging effect of the electric field leaking in free space at the output of the channel. The distribution function of those electrons both in angle and energy depends on the channel diameter, the gain of the MCP and the voltage applied to it. The few measurements that have been reported thus far in literature [18] show an energy range of those electrons of a few electron volt to more than 200 eV. Work is in progress at CETP to improve the characterization of these distribution functions that have a significant influence on high resolution detector performances. As is classically done

in all MCP-based imaging detectors, the divergence of the electrons is tentatively limited by proximity focusing with a large accelerating voltage and a small gap between the back face of the MCP and the collector. For safety reasons we have decided to set the distance between the back face of the MCP and the collector to 0.2 mm. This number was chosen after taking into consideration possible deformation of the MCP due, in particular, to moisture absorption before the instrument is baked out, and, more importantly, the possible entry of very small cometary dust particles in the instrument which could short-circuit the back face of the MCP and the LEDA anodes causing damage.

In the primary mode of operation, the back face of the MCP is polarized between approximately −200 and −350 V relative to the LEDA anodes. The resulting energy of the electrons is thus in the range 200–500 eV and they can produce secondary electrons with an efficiency close to 1 for the high energy fraction. These secondary electrons are bent back towards the anodes by the electric field but, nevertheless, their diverging trajectories result in a spreading of the mass peak. This effect represents the main limitation of the

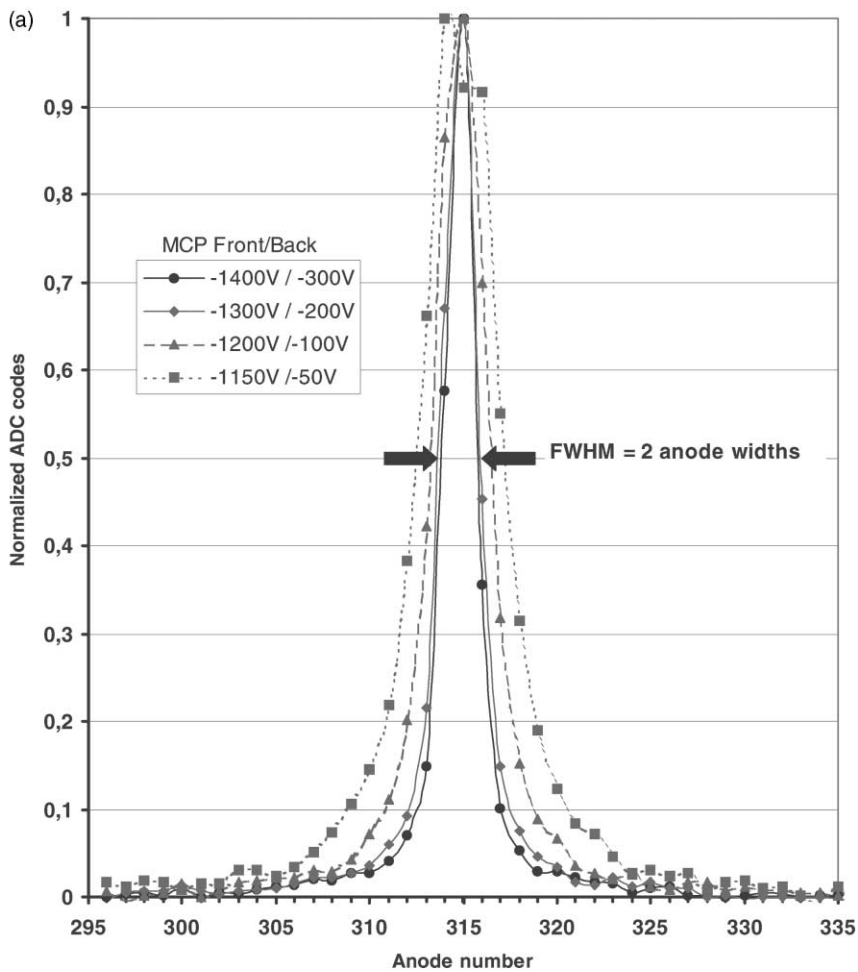

Fig. 3. Point spread function of the imaging detector in the primary mode of operation: (a) linear scale, (b) logarithmic scale, (c) measured peak and simulated peak corresponding to the CO/N_2 separation.

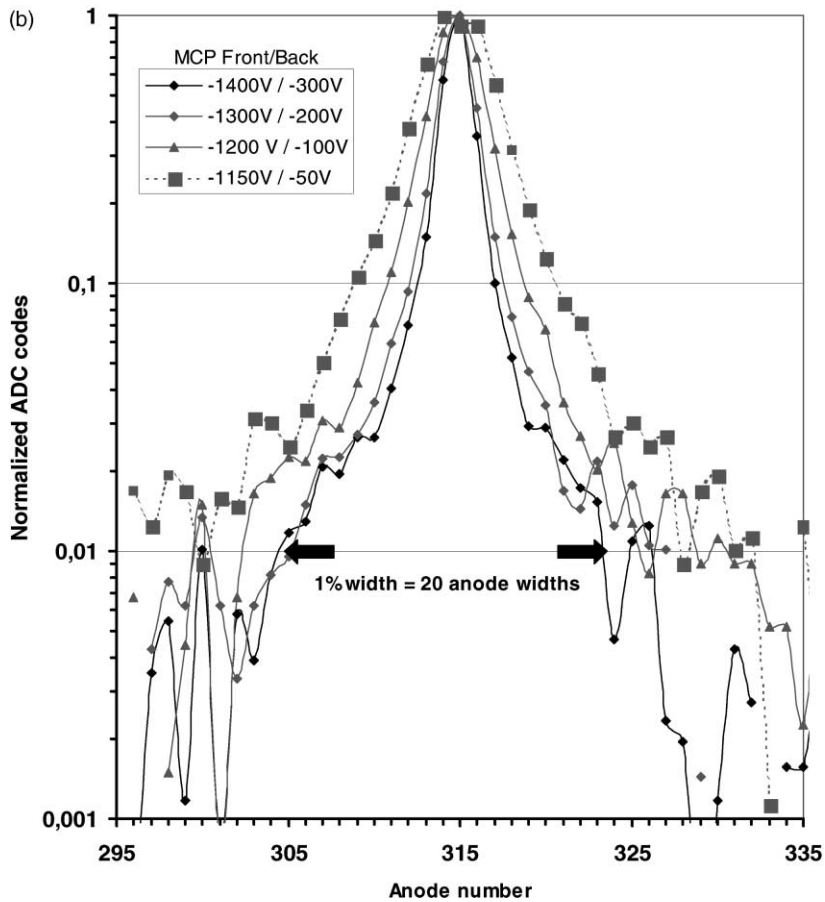

Fig. 3. (*Continued*)

effective mass resolution of the detector. An example of the variation of the point spread function of the detector as a function of the accelerating voltage between the MCP back face and the LEDA is shown in Fig. 3(a) and (b). It was obtained during laboratory tests of the prototype of the detector by using a low energy 600 eV ion beam and a 10 μm wide slit positioned 50 μm above the front face of the MCP. The effect of the electron acceleration voltage is clearly seen on the peak shape, particularly between 50 and 200 V with a peak width at 10% decreasing from 300 to 150 μm. The improvement starts to be very modest above 300 V which was selected as the operating voltage in the primary mode. At this voltage, the peak width at 1% of the point spread function is about 250 μm which must be compared with the distance between the two peaks of CO and N_2 of 350 μm. These two numbers clearly show that the detector meets the specifications of mass resolution and will ensure the detection of these two constituents even if their density ratio is of the order of 100. During testing the ion beam intensity was low and this is the reason why below the 1% level, the fluctuations of the signal start to mask the large scale variation of the point spread function which, nevertheless, seems to widen very significantly below this level.

At very low ion fluxes, the MCP is operated near the maximum gain of $\sim 5 \times 10^6$ and a charge of

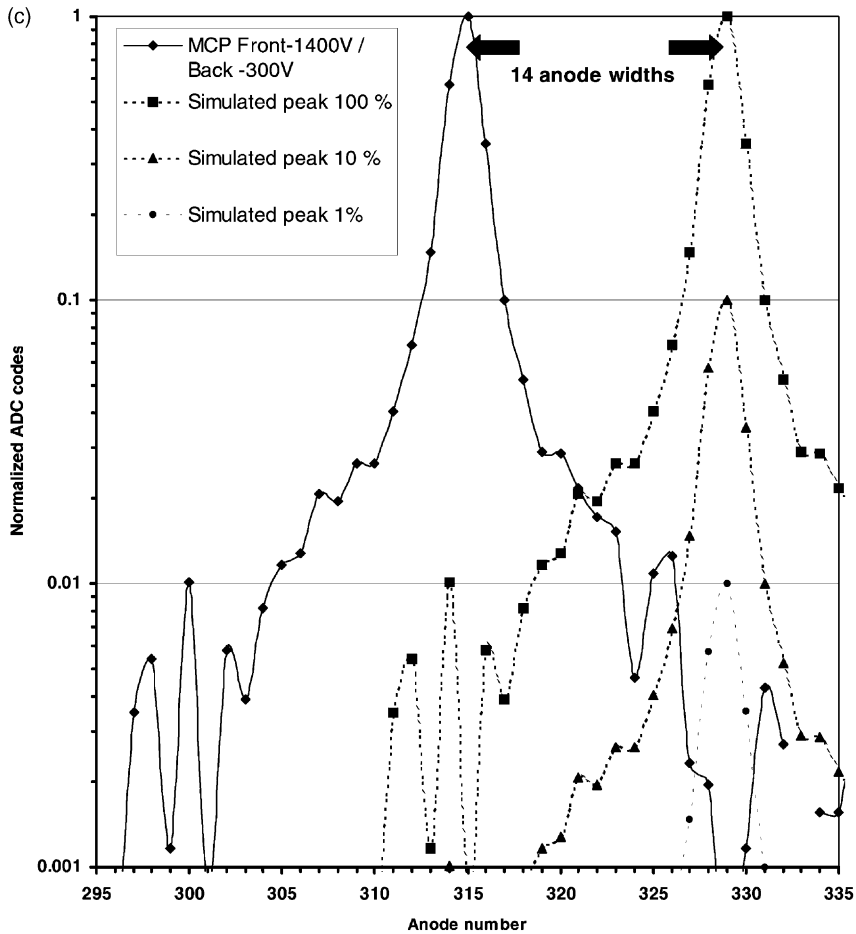

Fig. 3. (*Continued*)

$\sim 8 \times 10^{-12}$ C is spread over the LEDA with at least $\sim$40% on two pixels. A charge of 1.6×10^{-12} C on one pixel is about two orders of magnitude above the noise threshold of the LEDA electronics. Single electron pulses can therefore be detected and counted individually without problem provided that the reading times are short enough or the ion flux low enough so that only one pulse can occur on a mass peak during an integration time. This provides a sensitivity much higher than required by specifications and only limited by the MCP noise, which is typically of the order of 1 count/(cm^2 s) corresponding to $\sim 10^{-3}$ counts/(mass peak s).

5. Conclusion

In its present state the detector system installed in the focal plane of the DFMS instrument, which will be flown on the Rosetta orbiter, provides a satisfactory answer to the scientific requirements of the experiment. The imaging detector, composed of a MCP followed by a specifically designed ASIC circuit is the central part of this detector system; the ASIC consists of a CMOS chip, the LEDA 512, containing a multi-anode collector and its integrated electronics and of a ceramic chip carrier. Three main characteristics had to be demonstrated—sensitivity, dynamical range

and mass resolution—whilst the overall system had to take into account the requirements of reliability and in-flight verification of performances.

Reliability and assessment of in-flight performances were addressed by adding two more detectors. The CEM can be used in a way very similar to the imaging detector but, evidently, with a much reduced time resolution which, in particular, might hamper a precise comparison of different constituents. The Faraday cup allows direct measurement of the ion current of the neutral or ionized water peak and thus provide an absolute calibration, all the other masses being calibrated relative to water.

The basic concept of the imaging detector allows operation of the MCP over all its gain characteristics and thus in the pulse (saturated) mode and in an analog mode. When the ion fluxes are low, the MCP is operated at full voltage in the pulse mode and the imaging detector has a sensitivity well beyond that required: this will allow study of the neutral coma of comet Wirtanen during its very first stage of development with an atmosphere with a pressure about 10^{-15} Pa. Since the MCP can also be operated in an analog mode and its effective gain can be varied by more than seven orders of magnitude, the total dynamical range of the imaging detector, including an instantaneous range of more than 10^3 for the LEDA itself, meets the requirement.

The mass resolution was the most challenging question to be answered in particular due to safety limits

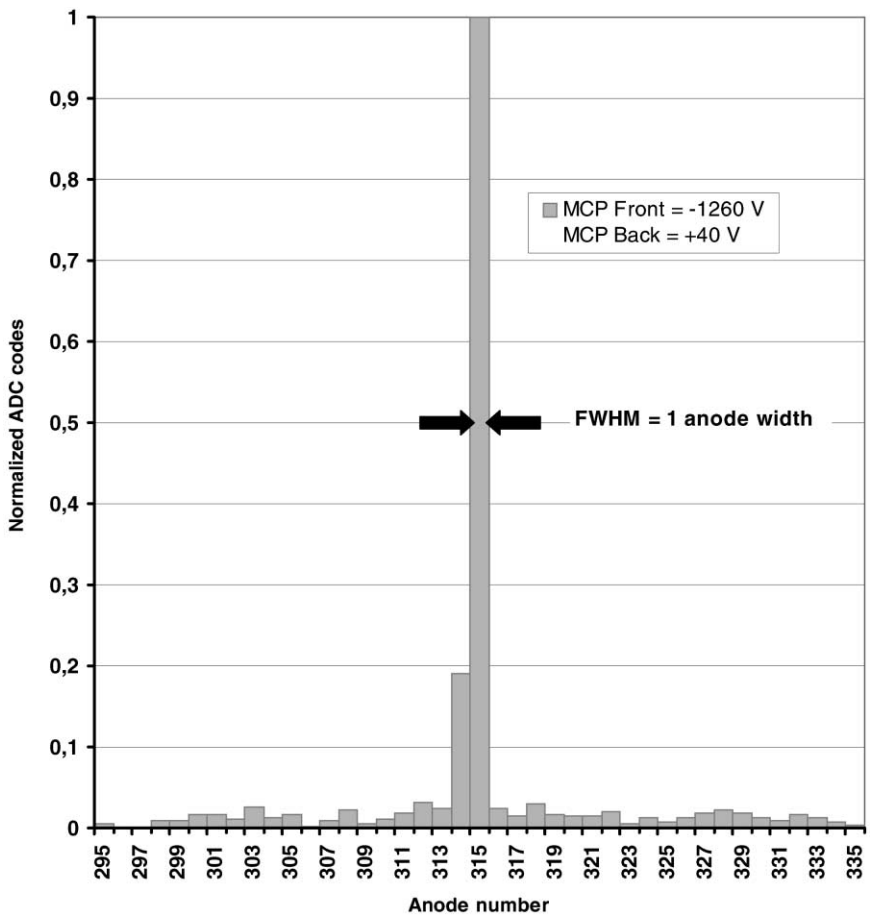

Fig. 4. Point spread function of the imaging detector in the “high resolution” mode of operation.

imposed on the minimum distance between the back of the MCP and the LEDA surface. The point spread function which has been measured during tests of the prototype has been shown to provide a mass resolution of ∼2500 at the 1% level that will allow separation of CO from N_2 and thus enable reliable measurements of rare isotopes such as ^{13}C, which will be distinguishable from ^{12}CH.

6. Future work

In the course of the development and testing of the prototype we have found an innovative way to improve the performances of the imaging detector which we just want to mention briefly in this paper as an indication of likely improvements for the future. The limitation of the performances of the primary mode of operation with a large negative potential on the back face of the MCP results from the secondary emission following the impact of MCP electrons: these secondary electrons are repelled by closely located anodes, which widens the focal image on the collector. Our idea was to get rid of the collection of all secondaries by preventing them from impinging on the detector. This can be achieved by applying on the back face of the MCP, a voltage positive with respect to the LEDA; tests have shown that voltages from +20 to +60 V are sufficient. In our case, both the typical energies of the MCP electrons and the emission properties of the surface material of the LEDA anodes (TiN) are such that the flux of secondary electrons emitted by the anodes is larger than the flux of the primary MCP electrons; the net result is thus a positive charge deposited on the anodes with an amplitude which is about 5% of that of the negative charge in the primary mode of operation. This positive charge can still be measured by the LEDA since this component can operate with charges of either sign, although in its present version, the dynamics is reduced by a factor of 2.5 in the case of positive charges. Fig. 4 provides an example of data obtained under similar conditions as in Fig. 3: the point spread function is significantly reduced down to about 2–3 pixels at the 1% level. A more detailed description and modeling of the operation of the imaging detector in this “high resolution” mode will be the subject of a forthcoming paper.

Acknowledgements

We want to thank P. Eberhardt and J. Fisher of the Physikalisches Institut of the University of Bern for valuable assistance in the course of this study. This work was supported on the French side by means of a contract CNES/Rosetta/98-70 granted by CNES, the French Space Agency, and on the Belgian side through funding by the European Space Agency PRODEX Office in the framework of the ROSINA project approved by the Belgian Federal Office for Scientific, Technical and Cultural Affairs (DWTC-SSTC).

References

[1] G. Schwehm, R. Schulz, Space Sci. Rev. 90 (1999) 313.
[2] H. Balsiger, K. Altwegg, E. Arijs, J.L. Bertaux, J.J. Berthelier, B. Block, P. Boschler, G.R. Carignan, L. Duvet, P. Eberhardt, B. Fiethe, J. Fischer, L.A. Fisk, S.A. Fuselier, A.G. Ghielmetti, F. Gliem, T.I. Gombosi, J.M. Illiano, T. Koch, E. Kopp, A. Korth, K. Lange, H. Lauche, S. Livi, A. Loose, T. Magoncelli, C. Mazelle, M. Mildner, E. Neefs, D. Nevejans, H. Reme, J.A. Sauvaud, S. Scherer, A. Schoenemann, E.G. Shelley, J.H. Waite, C. Westerman, B. Wilken, J. Woch, H. Wolnik, P. Wurz, D.T. Young, ESA Monograph SP-1165, 2001, in press.
[3] J.P. Lebreton, Models of Neutral and Ionized Gas Densities in the Coma of Comet Wirtanen, 1995 (unpublished report).
[4] T.I. Gombosi, D.L. De Zeeuw, R.M. Häberli, K.G. Powell, J. Geophys. Res. 101 (1996) 15233.
[5] J.G. Timothy, Rev. Sci. Instrum. 46 (1975) 1615.
[6] A.L. Broadfoot, B.R. Sandel, Appl. Opt. 16 (1977) 1533.
[7] M. Lampton, C.W. Carlson, Rev. Sci. Instrum. 50 (1979) 1093.
[8] H. Keller, G. Klingelhöfer, E. Kankeleit, Nucl. Instrum. Meth. 258 (1987) 221.
[9] J.S. Lapington, A.D. Smith, D.M. Walton, H.E. Schwarz, IEEE Trans. Nucl. Sci. 34 (1987) 431.
[10] T. Daud, J.R. Janesick, K. Evans, T. Elliott, Opt. Eng. 26 (8) (1987) 686.
[11] K. Birkinshaw, Trans. Inst. Meas. Control 16 (1994) 149.
[12] K. Birkinshaw, D.P. Langstaff, Int. J. Mass Spectrom. Ion Processes 132 (1994) 193.
[13] K. Birkinshaw, Int. J. Mass Spectrom. Ion Processes 33 (1998) 64.

[14] D.J. Narayan, D.P. Langstaff, K. Birkinshaw, Int. J. Mass Spectrom. Ion Processes 149/150 (1998) 439.
[15] J.J. Berthelier, J.M. Illiano, R.R. Hodges, J. Covinhes, M. Godefroy, G. Gogly, J. Guillou, F. LeGoff, F. Leblanc, Z. Racic, P. Rouchette, D. Krankowsky, D. Dörflinger, O. Vaisberg, V. Smirnov, N. Kolesova, Measurements Techniques in Space Plasmas, AGU Monograph 103, 1998, p. 215.
[16] D. Krankowsky, P. Lämmerzhal, D. Dörflinger, I. Herrwerth, U. Stubbemann, J. Woveries, P. Eberhardt, U. Dolder, J. Fisher, U. Herrmann, H. Hofstetter, M. Jungck, F.O. Meier, W. Schulte, J.J. Berthelier, J.M. Illiano, M. Godefroy, G. Gogly, P. Thevenet, J.H. Hoffmann, R.R. Hodges, W.W. Wright, ESA Monograph SP-1077, 1986, p. 109.
[17] D. Nevejans, E. Neefs, S. Kavadias, P. Merken, C. Van Hoof (companion paper in this issue).
[18] I.M. Bronshteyn, A.V. Yevdokimov, V.M. Stozharov, A.M. Tyutikov, Radio Eng. Electron. Phys. 24 (1980) 150.